Relativistic, Electromagnetic Waves in Pulsar Winds

O. Skjæraasen

Institute of Theoretical Astrophysics, University of Oslo, PO Box 1029 Blindern, N-0315 Oslo, Norway. email: olafsk@astro.uio.no

Abstract

We study extremely nonlinear, coherent electromagnetic waves in the context of relativistic, expanding plasma flows, where a confining external medium triggers the formation of a shock. Using a combination of analytical methods and Particle-In-Cell simulations, we look at mechanisms of wave generation and dissipation, as well as how the waves affect the particle distribution. For a large-amplitude wave of general polarisation, any given set of wave parameters uniquely fixes the particle and energy flux associated with the flow. In cases where the wave properties can be constrained, this can be used to estimate the flow parameters. The prime application of our work is to pulsar winds and their termination shocks, where it provides a viable alternative to magnetohydrodynamic models.

The Wavelike Pulsar Wind

Pulsar winds are believed to carry most of their energy in the form of Poynting-flux close to the pulsar, but to be particle-dominated at the termination shock (Kennel & Coroniti, 1984; Arons, 2002; Lyubarski, 2003). The question of how the Poynting flux of the wind is dissipated has been subject to considerable debate in recent years.

A central issue in the discussion is the fate of the highly nonlinear wave which is launched into the expanding wind by the spinning pulsar motion (i.e., in the general case where the neutron star spin and magnetic dipole axes are non-parallel). The behaviour of the wavelike wind has been studied in numerous works, usually from a magnetohydrodynamics (MHD) point of view. It is clear, however, that ideal MHD cannot apply to arbitrarily large radii, since the diverging wind motion dilutes the plasma until the flux-freezing condition breaks down, at a critical radius r_c which is poorly constrained, but is thought to be in the inner wind, although well beyond the light cylinder. For radii $r > r_c$, magnetic reconnection might set in (Coroniti, 1990; Michel, 1994; Lyubarsky & Kirk, 2001; Kirk & Skjæraasen, 2003), leading to a radial decrease in the ratio σ of Poynting flux to particle energy flux, and possibly producing an observable signature in the form of pulsed X-rays and γ-rays (Arons 1979, Kirk et al., 2002; Skjæraasen, 2004; Petri & Kirk, 2005).

In the current project, we explore an alternative to the MHD-based models: Beyond r_c, the carrier wave of the wind might be a relativistically nonlinear, electromagnetic wave (Melatos & Melrose, 1996; Melatos, 1998). This non-MHD scheme finds support in that the displacement current dominates the particle current by a large factor at large radii. We use analytical methods and Particle-In-Cell simulations to determine the state of the TEM wave as it propagates in the wind zone from $r \approx r_c$ to the termination shock and beyond.

Nonlinear TEM Waves

A nonlinear electromagnetic wave can propagate even if its frequency ω_0 is less than the effective plasma frequency. For circularly polarized, purely transverse electromagnetic (TEM) waves in a cold plasma with a relativistic drift speed v_d and a DC magnetic field B_0, both in the direction of wave propagation, the plane wave dispersion relation is

$$\frac{1}{\beta^2} = 1 - \frac{\omega_\dagger^2}{\omega_0^2}\left[\frac{1}{\gamma^+ + \hat{B}/R} + \frac{1}{\gamma^- - \hat{B}/R}\right], \quad (1)$$

where $\eta = ck/\omega_0$ is the index of refraction, $\omega_\dagger = \sqrt{n^\pm e^2/\epsilon_0 m}$, $\gamma^\pm$ and $n^\pm$ are the (positron, electron) bulk Lorentz factor and lab-frame density, $R = 1 - \eta v_d/c$ is the Doppler factor, $\hat{B} \equiv eB_0/m\omega_0$, and $\hat{E}$ is a dimensionless amplitude defined by $\hat{E} = eE_0/mc\omega_0$, where E_0 is the physical electric field amplitude. In the unmagnetised limit, $B_0 \to 0$, the dispersion relation becomes (Akhiezer & Polovin, 1956) $\eta^2 = 1 - 2(\omega_p^2/\omega_0^2)/(1+\hat{E}^2)^{1/2}$, where $\omega_p = \sqrt{n^\pm e^2/\epsilon_0 m\gamma^\pm}$, Using PIC simulations, we have verified this dispersion relation to within 5 per cent for $\hat{E} \gg 1$ and $\gamma_b \gg 1$.

Application to the Crab

We find that (i) the coupling between the inner and outer parts of the Crab wind is nontrivial, and corresponds to a transition from subluminal to superluminal wave propagation; (ii) at the termination shock, the TEM wave modulates the particle distribution and causes anisotropic, polarisation-dependent heating; (iii) after the wave encounters the shock, its amplitude is reduced by 99 per cent over a length scale of $10^2 - 10^3$ plasma skin depths; (iv) the ultimate fate of the wave is controlled by microphysical wave-wave and wave-particle interactions, and ultimately it might propagate as a linear wave.

For the Crab pulsar wind termination shock, we analytically obtain $\sigma \simeq 9.0 \times 10^{-3}$, $\hat{E} \simeq 2.5$, and $1 - \eta \simeq 4.8 \times 10^{-11}$, using canonical Crab parameters. The very slight deviation of η from unity reflects the fact that the displacement current dominates the particle current by many orders of magnitude. The angle over which the wave decays exceeds $0.05''$, and causes a latitude-dependent (i.e., polarisation-dependent), anisotropic heating of the shocked plasma, with a possible observable signature in optical and X-rays (Skjæraasen, Melatos, & Spitkovsky, ApJ 634, 542, 2005).

PIC-Simulations of Wind's Termination Shock

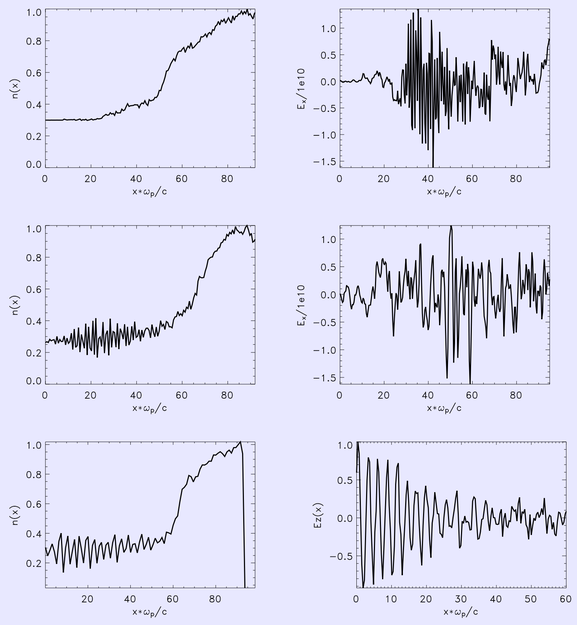

Fig 1. Top: Hydrodynamic ($\sigma = 0$) shock. At $t = 0$, a cold beam has been launched with 4-velocity $(\gamma_b c, u_x, u_y, u_z) = (3900c, 3900c, 0, 0)$ from $x = 0$, propagating towards right (larger x). After reflecting off a wall at $x\omega_p/c \simeq 94$, the beam has destabilized, forming a left-moving shock via the Weibel instability. The left and right plots show the density profile and the longitudinal field component E_x across the shock. The upstream, precursor, and shock interior regions correspond roughly to $x\omega_p/c < 40$, $20 < x\omega_p/c < 40$, $40 < x\omega_p/c < 80$. **Middle: Shock with Circularly Polarized TEM Wave ($\sigma = 6.0$) in Unmagnetized Plasma ($\hat{B} = 0$).** The TEM wave couples nonlinearly to longitudinal oscillations, which lead to density fluctuations upstream. The wave decays over a scale of some $100\omega_p/c$. **Bottom: Shock with Linearly Polarized Transverse-Longitudal Wave in Unmagnetized Plasma ($\sigma = 6.4$ and $\hat{B} = 0$).** At left, the density profiles of electrons and positrons are plotted separately (solid/dotted lines), but overlap almost exactly. Note the strong, coherent density oscillations in the upstream and precursor; unlike the case for the TEM wave. At right, E_z is shown, and the characteristic sawtooth shape of a linearly polarized relativistic EM wave is evident in the precursor.

Shock Jump Conditions

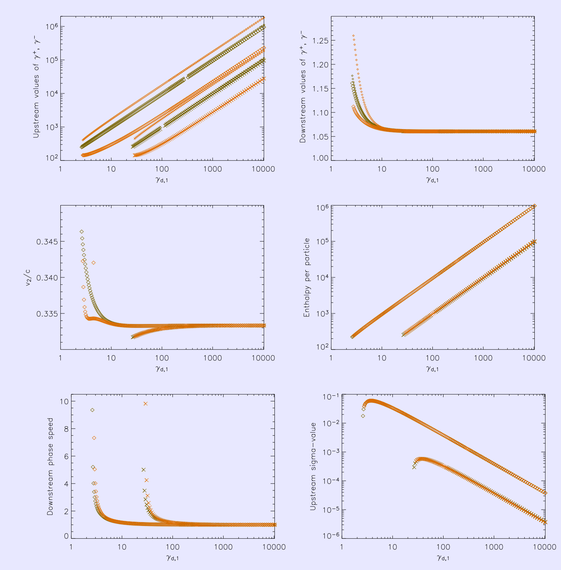

Fig. 3. RANKINE-HUGONIOT SOLUTIONS FOR SUPERLUMINAL TEM WAVE ENCOUNTERING SHOCK IN MAGNETIZED PLASMA. Top left: Upstream bulk Lorentz factors for electrons (small symbols) and positrons (large symbols), as a function of upstream drift speed $\gamma_{d,1}$. **Top right**: Downstream Lorentz factors. **Center left**: Downstream drift speed (units of c). **Center right**: Downstream enthalpy per particle (units of mc^2). **Bottom left**: Downstream wave phase speed (units of c). **Bottom right**: Upstream σ-value (ratio between Poynting flux and kinetic energy flux). For these parameters, the downstream σ is almost unchanged. Parameters: $\omega/\omega_p = 0.088$ together with DC-fields $\hat{B} \equiv eB_0/m\omega = 10$ (brown) or $\hat{B} = 100$ (orange), and wave amplitudes $\hat{E} \equiv eE_0/mc\omega = 10$ (crosses) or $\hat{E} = 100$ (diamonds). Outer Crab wind parameters correspond roughly to the rightmost region of each plot (for best illustrating parameter dependencies, ω/ω_p has been set artificially low here).

Encounter of Linearly Polarized Wave with Termination Shock

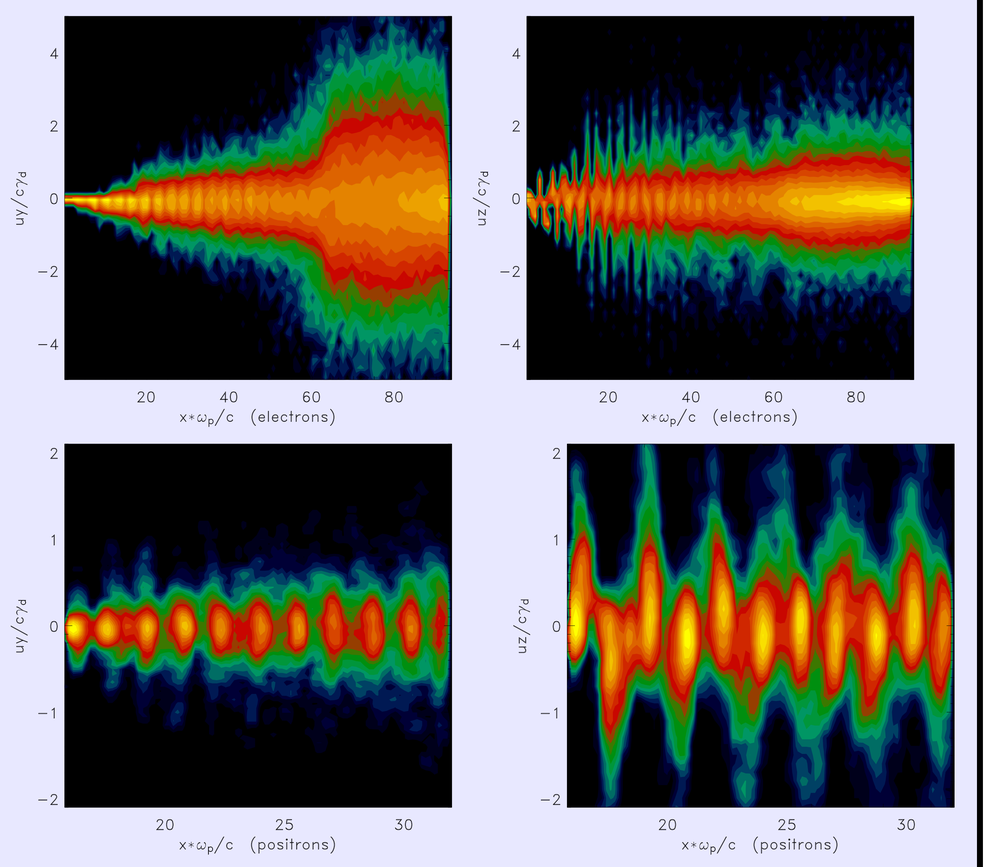

Fig 2. LINEARLY POLARIZED WAVE MODULATIONS OF SHOCK IN UNMAGNETIZED PLASMA ($\sigma = 6.4$ and $\hat{B} = 0$). At $t = 0$, a cold electron-positron beam ($\gamma_d = 3900$) and a linearly polarized EM wave (with $\omega_0/\omega_p = 1.97$, $\hat{E}_x = \hat{E}_y = 0$, and $\hat{E}_z = 5.0 \times 10^3$) have been launched from $x = 0$. Away from $x = 0$, the actual (local) σ-value quickly drops far below the initial value ($\sigma = 6.4$), as the antenna field couples to the plasma and forms a nonlinear sawtooth-like wave At $x\omega_p/c \approx 95$, a left-moving shock has been produced (as in Fig. 1). In a hydrodynamic shock ($\sigma = 0$), there would be a gradual broadening of the distribution, without the bunched, oscillatory patterns seen here. **Top left**: Global distribution of electrons in (x, u_y). The positron distribution is similar. **Top right**: Global distribution of electrons in (x, u_z). The u_z-component of the 4-velocity couples directly to the wave. **Bottom left**: Local distribution of positrons in (x, u_y) in the precursor. Note the strong bunching of particles along the x-axis. The electron distributio is similar. **Bottom right**: Local distribution of positrons in (x, u_z) in the precursor. Again, note the strong bunching of particles along the x-axis, as well as the oscillatory displacement from $u_z = 0$ induced by the wave. For the electrons, this displacement is opposite at all x.

Decay of TEM Wave in Shock Interior

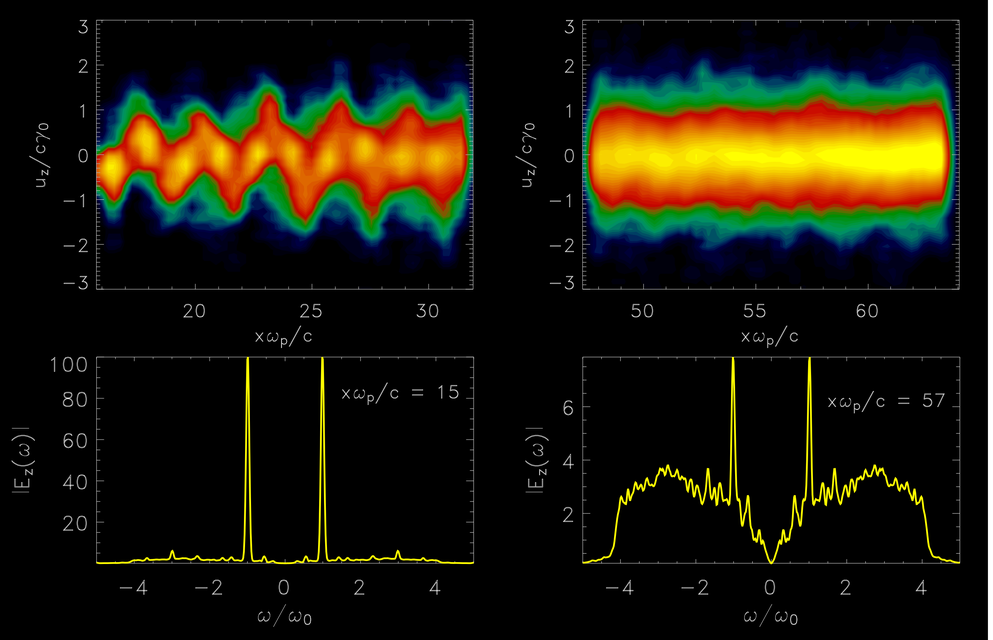

Fig 4. CIRCULARLY POLARIZED WAVE MODULATIONS OF SHOCK IN UNMAGNETIZED PLASMA ($\sigma = 2.0$ and $\hat{B} = 0$). **Top row**: Positron density in (x, u_z)-space for (left) $10 < x\omega_p/c < 20$ and (*right*) $20 < x\omega_p/c < 30$. At top left, the particles are strongly phase-coherent with the TEM wave (which has a wavelength of $\approx 3.3c/\omega_p$), although thermal broadening can be seen at $x\omega_p/c > 11$. At top right, the thermal width is larger than the quiver amplitude, but a periodic modulation is still evident. (In the absence of the wave, one gets a straight beam centered on $u_z = 0$, gradually broadening with $x\omega_p/c$). **Bottom row**: Frequency spectrum $|E_y(\omega)|$ at (*left*) $x\omega_p/c = 14$ and (*right*) $x\omega_p/c = 29$, obtained soon after the shock is developed. The lines at $\omega = \pm\omega_0$ are the TEM wave. As $x\omega_p/c$ increases, the lines decay while the thermal background grows. Parameters used: At the launch point ($x = 0$), the ratio between the Poynting and kinetic energy fluxes is $\sigma_0 = 2.0$, the drift Lorentz factor is $\gamma_b = 3870$, the ratio between the wave and plasma frequencies is $\omega_0/\omega_p = 1.97$, and $\hat{E}(x = 0) = 2.0 \times 10^3\sqrt{\sigma}_0$.